Earth Surf. Dynam. Discuss., 1, 923–950, 2013
www.earth-surf-dynam-discuss.net/1/923/2013/
doi:10.5194/esurfd-1-923-2013

Earth Surface Dynamics Discussions
Open Access

Effect of self-stratification on sediment diffusivity in channel flows and boundary-layers: a study using Direct Numerical Simulations

S. Dutta[1], M. I. Cantero[3], and M. H. Garcia[1,2]

[1]Dept. of Civil and Environmental Engineering, University of Illinois at Urbana-Champaign, Urbana, USA
[2]Dept. of Geology, University of Illinois at Urbana-Champaign, Urbana, USA
[3]Centro Atómico Bariloche and Instituto Balseiro, Consejo Nacional de Investigaciones Científicas y Técnicas (CONICET) and Comisión Nacional de Energía Atómica (CNEA), San Carlos de Bariloche, Río Negro, Argentina

Received: 28 October 2013 – Accepted: 31 October 2013 – Published: 19 November 2013

Correspondence to: S. Dutta (dutta5@illinois.edu)

Published by Copernicus Publications on behalf of the European Geosciences Union.

Abstract

Sediment transport in nature comprises of bed-load and suspended load, and precise modelling of suspended load transport is essential for accurate sediment flux estimation. Traditionally, non-cohesive suspended sediment has been modelled using the advection-diffusion equation (Garcia, 2008), where the success of the model is largely dependent on accurate approximation of the sediment diffusion coefficients. The current study explores the effect of self-stratification on sediment diffusivity using suspended sediment concentration data from Direct Numerical Simulations (DNS) of flows subjected to different levels of stratification, where the level of stratification is dependent on the particle size (parameterized using particle fall velocity $\tilde{V}$) and volume-averaged sediment concentration (parameterized using shear Richardson number Ri_τ). Two distinct configurations were explored, first the channel flow configuration (similar to flow in a pipe or a duct) and second, a boundary layer configuration (similar to open-channel flow). Self-stratification was found to modulate the turbulence intensity (Cantero et al., 2009), which in turn was found to reduce vertical sediment diffusivity in portions of the domain exposed to turbulence damping. Effect of particle size on vertical sediment diffusivity has been studied in the past by several authors (Rouse, 1937; Coleman, 1970; Nielsen and Teakle, 2004); so in addition to the effect of particle size, the current study also explores the effect of sediment concentration on vertical sediment diffusivity. The results from the DNS simulations were compared with experiments (Ismail, 1952; Coleman, 1986) and field measurements (Coleman, 1970); and were found to agree qualitatively especially for the case of channel flows. The aim of the study was to understand the effect of stratification due to suspended sediment on vertical sediment diffusivity for different flow configurations, in order to gain insight of the underlying physics, which will eventually help us to improve the existing models for sediment diffusivity.

ESURFD

1, 923–950, 2013

1 Introduction

Turbulent mixing and accompanying transport is a prevalent phenomenon in natural and industrial settings. One of the most important transport phenomena in nature is that of sediment, and it can be broadly divided into bed-load transport and suspended load transport. In most rivers, suspended load comprises of around 80–85 percentage of the total sediment load, thus playing an important role in morphodynamics of the system. In-situ measurement of suspended sediment is still very discontinuous and expensive, so accurate modelling of transport of suspended sediment is essential for correct approximation of the net sediment flux in a river. For the generic case of suspended sediment of constant density and particle size in unsteady turbulent flow, suspended sediment can be modelled using the Reynolds averaged mass balance equation and the appropriate boundary conditions (Garcia, 2008).

$$\frac{\partial \bar{c}}{\partial t} + \frac{\partial F_i}{\partial x_i} = 0, \quad \text{where} \quad F_i = (u_i - V\delta_{i3})\,\bar{c} + \overline{u_i' c'} \tag{1}$$

$\bar{c}$ is the mean (averaged over turbulence) volumetric concentration of suspended sediment, c' is instantaneous fluctuation of sediment concentration, u_i is the mean fluid velocity, u_i' is turbulent fluctuations, F_i is the Reynolds averaged suspended sediment flux, V is particle settling velocity in quiescent water and δ_{i3} is the Kronecker delta. With the assumption of the river/stream flowing in steady state and being confined in a wide channel, Eq. (1) reduces to (Garcia, 2008)

$$\frac{\mathrm{d}}{\mathrm{d}z}\left(\overline{w'c'} - V\bar{c}\right) = 0. \tag{2}$$

Under typical conditions prevailing in most streams and rivers, the suspended sediment can be safely assumed to be in equilibrium; and combining it with the boundary conditions at free surface, Eq. (2) further reduces to $\overline{w'c'} - V\bar{c} = 0$. The eddy-diffusivity assumption can be used to model $\overline{w'c'}$; the resulting relationship has been widely used

ESURFD
1, 923–950, 2013

for modelling transport of suspended sediment (Rouse, 1937; Vanoni, 1946):

$$K_z \frac{\mathrm{d}\bar{c}}{\mathrm{d}z} + V\bar{c} = 0, \tag{3}$$

where K_z is the vertical sediment diffusivity due to turbulence mixing. Success of the above model depends on the correct estimation of the sediment diffusivity coefficient. Using Prandtl analogy, and assuming that the logarithmic velocity profile holds for the full depth of the flow, Rouse (1937) derived a formula for K_z

$$\frac{K_z}{Hu_*} = \kappa \frac{z}{H}\left(1 - \frac{z}{H}\right). \tag{4}$$

In the above equation H is depth of the flow, κ von Karman constant, u_* is the bed shear velocity and z the normal distance from the bed. Even though Prandtl's analogy might not perfectly hold under all circumstances, the above relation (also known as the Rousean formulation for vertical eddy viscosity) has been used extensively in the field of suspended sediment transport. One of the first studies to question the universal applicability of the Rousean formulation was Coleman (1970); he used suspended sediment measurements from lab experiments and field measurements to calculate K_z/Hu_* for sands with different values of V/u_*. Rearranging Eq. (3) and dividing both sides by Hu_* gives us the formula used for calculating K_z/Hu_*

$$\frac{K_z}{Hu_*} = -\frac{\tilde{\bar{c}}\tilde{V}}{\mathrm{d}\tilde{\bar{c}}/\mathrm{d}\tilde{z}}. \tag{5}$$

In the above equation $\tilde{V}$ is V/u_*, $\tilde{z}$ is z/H and $\tilde{\bar{c}}$ is the mean volumetric suspended sediment concentration. Coleman (1970) in his study used field data of Anderson (1942) to calculate K_z/Hu_*, and the same data has been reproduced here (Fig. 1) along with the Rousean profile calculated using Eq. (4). We can observe in Fig. 1, that only in the lower portion of the domain K_z/Hu_* is parabolic and for most cases the Rousean profile underestimates vertical sediment diffusivity. Van Rijn (1984) put forward the idea

ESURFD
1, 923–950, 2013

that the ratio of sediment diffusivity and kinematic eddy diffusivity (one we get form Eq. 4) is always greater than 1 and suggested the use of an empirical coefficient to adjust kinematic eddy diffusivity to match the vertical sediment diffusivity. On the contrary Bennett et al. (1998) attributed the disparity to the use of suspended sediment concentration profile to calculate sediment diffusivity, instead of using direct turbulence measurements. In general, the common consensus is that the Rousean profile is not an appropriate surrogate for vertical sediment diffusivity. The issues stem from the break down of Prandtl's analogy, due to the inertial effects of relatively large sediment particles (Nielsen, 1992). This was behaviour was actually observed by Rouse (1938) in his classic turbulence jar experiments.

The Rousean profile, though a very good first approximation, does not capture completely the ingrained physics present in the interaction of suspended sediment and its ambient fluid. Nielsen and Teakle (2004) have used finite-mixing-length theory to justify their interpretation of Coleman's (1970) data, in which they point out that vertical sediment diffusivity of sediment increases with increase in V/u_* (dubbed the Rouse number, though exact definition of Rouse number is $V/\kappa u_*$). If we observe Fig. 1, in which we have reproduced data from Coleman (1970); a trend emerges where K_z/Hu_* for cases with higher V/u_* is higher than those with lower V/u_*. But the aforementioned trend is not very prominent, and there are cases (e.g. between 0.585 and 0.696) where the sediment with relatively lower V/u_* has higher or almost equal sediment diffusivity than the sediment with relatively higher V/u_*. This may be an artefact of us not recognizing all the embedded physics.

Our hypothesis is that the anomaly can be explained if we also take the effect of self-stratification caused by the suspended sediment into consideration. The settling sediment particles form a continuous concentration profile, with higher concentration near the bottom and lower at the top. This concentration gradient causes stratification in the fluid, and as the suspended sediment particles themselves cause stratification, the phenomenon is also referred as self-stratification. This concentration gradient is known to modulate turbulence and affect bulk properties of the flow (Cantero et al., 2009,

ESURFD
1, 923–950, 2013

2012; Shringarpure et al., 2012). Wright and Parker (2004) showed the importance of sediment-induced stratification in large low-gradient streams/rivers. Smith and McLean (1977) and then others, proposed the use of simple algebraic closures based on the gradient Richardson number (Ri_g) to take into account the effect of self-stratification on the Rousean profile.

Aim of the present study is to explore the effect of self-stratification on vertical sediment diffusivity under two different configurations; first for channel flows, which is an analogue for flow in a pipe or a duct and second for a boundary layer configuration, which is similar to an open-channel flow. For the first portion of the study, we have used steady state sediment concentration profiles from Direct Numerical Simulations (DNS) of sediment-laden flows. For the DNS, sediment has been modelled using an Eulerian approach and the sediment particles do not have any inertia. Though this is not true for most sediment in nature, it was done in order to explore the effect due to self-stratification without other physics (like inertial effects, see for example Cantero et al., 2008) coming into play. DNS was done for a constant shear Reynolds number (Re_τ) but for different levels of self-stratification, which depend on the particle settling velocity (parameterized using $\tilde{V} = V/u_*$) and volume-averaged suspended sediment concentration (parameterized using shear Richardson number Ri_τ). Traditionally, sediment diffusivity under different circumstances have been only studied for the open-channel like configuration; so we think the present study is one of the first studies to explore it in the channel-flow setting. Apart from using data from DNS, we have also used data from experiments by Ismail (1952) and Coleman (1986) to study the effect of stratification on sediment diffusivity. The aim of the current study is to extend our understanding of the effects of self-stratification on sediment diffusivity in turbulent channel and open-channel like flows.

ESURFD
1, 923–950, 2013

2 Mathematical formulation

Direct Numerical Simulations (DNS) were conducted for a horizontal channel, where the flow is driven by a constant pressure gradient. The constant pressure gradient here is a surrogate for a constant slope in a stream/river that drives the flow, especially for the open-channel like configuration. Suspended sediment particles are assumed to be of constant size, negligible inertia, and having a constant settling velocity $\tilde{V}$. Eulerian representation was used to represent the suspended sediment particles, and this has been found to be valid for sediment particles that are small enough (Ferry and Balachandar, 2001). The flow is assumed to be dilute for Boussinesq approximation to hold. The set of dimensionless equations used to model the flow is

$$\frac{\partial \tilde{u}_i}{\partial \tilde{t}} + \tilde{u}_j \frac{\partial \tilde{u}_i}{\partial \tilde{x}_j} = \tilde{G}\delta_{i1} - \frac{\partial \hat{p}}{\partial \tilde{x}_i} + \frac{1}{Re_\tau}\frac{\partial^2 \tilde{u}_i}{\partial \tilde{x}_j \partial \tilde{x}_j} - Ri_\tau \left(\tilde{c} - \tilde{c}^{(\mathrm{h})}\right)\delta_{i3} \tag{6a}$$

$$\frac{\partial \tilde{u}_i}{\partial \tilde{x}_i} = 0 \tag{6b}$$

$$\frac{\partial \tilde{c}}{\partial \tilde{t}} + \left(\tilde{u}_j - \tilde{V}\delta_{i3}\right)\frac{\partial \tilde{c}}{\partial \tilde{x}_j} = \frac{1}{ScRe_\tau}\frac{\partial^2 \tilde{c}}{\partial \tilde{x}_j \partial \tilde{x}_j} \tag{6c}$$

In the above equations, $\tilde{u}_i$ is the velocity of the fluid phase, $\tilde{c}$ is the volumetric concentration of the suspended sediment particles and $\tilde{c}^{(\mathrm{h})}$ is the horizontally averaged suspended sediment concentration. $\tilde{G}$ is the constant streamwise pressure gradient driving the flow and has magnitude equal to 1. And $\hat{p}$ is the pressure field, which is the combination of the dynamic pressure ($\tilde{p}$) and the hydrostatic component due to the suspended sediment. The mathematical formulation used in the present study is exactly the same as the one used by Cantero et al. (2009) in their study of turbulence modulation due to self-stratification, and additional details about the model can be found in Cantero et al. (2009). In the above set of equations, all the variables are dimensionless. Velocity has been made dimensionless using average shear velocity

ESURFD
1, 923–950, 2013

(u_*); parameter used for scaling length is the channel half-height h (where $2h$ is the height of the channel) and parameter used for scaling pressure is $\rho_f u_*^2$, where ρ_f is ambient fluid density. Equation (6) has four dimensionless numbers, which together define various properties of the flow; shear Reynolds number (Re_τ), shear Richardson number (Ri_τ), Schmidt number (Sc) and the non-dimensional particle fall velocity ($\tilde{V}$). These non-dimensional numbers are defined as

$$Re_\tau = \frac{u_* h}{\nu} \qquad Ri_\tau = \frac{gRc^{(\upsilon)}h}{u_*^2}$$
$$Sc = \frac{\nu}{K_s} \qquad \tilde{V} = \frac{V}{u_*} \tag{7}$$

where ν is the kinematic viscosity, g is acceleration due to gravity, K_s is diffusivity of the sediment particles (this diffusion of sediments arise from their long range hydrodynamic interaction, see for example Segre et al., 2001), $c^{(\upsilon)}$ is the volume-averaged concentration, $R = \rho_s/\rho_f - 1$ and ρ_s is the density of the sediment particles. In the current study all the DNSs were done for $Re_\tau = 180$. Shear Reynolds number of the flow was kept constant, because our aim was to understand the effect of self-stratification, when the flow remains the same. Shear Richardson number (Ri_τ) is used to parameterize volume-averaged suspended sediment concentration ($c^{(\upsilon)}$), and it also plays an important role in influencing the final degree of self-stratification (Dutta, 2012). $\tilde{V}$ influences the degree of self-stratification by defining the sediment concentration profile for cases having constant Ri_τ (initial sediment concentration) and Re_τ (Cantero et al., 2009). Dutta (2012) showed that in addition to $\tilde{V}$, even Ri_τ has an effect on the final degree of self-stratification; so in the current study both $\tilde{V}$ and Ri_τ are varied to get different levels of self-stratification. Based on observations made in previous studies (Cantero et al., 2009) Schmidt number (Sc) was kept equal to 1.

The above stated governing equations were solved using a dealiased pseudo-spectral code. The setup is exactly the same as the one used by Cantero et al. (2009), so further details of the exact numerical methods adopted can be found there. Di-

ESURFD
1, 923–950, 2013

mensions of the horizontal channel used for the numerical simulations were $\tilde{L}_x = 4\pi, \tilde{L}_y = 4\pi/3$ and $\tilde{L}_z = 2$, and the channel was discretized using a grid of resolution $N_x = 96, N_y = 96$ and $N_z = 97$. This resolution has been found good enough to capture all the relevant length scales (Cantero et al., 2009). Periodic boundary conditions were used in the longitudinal and transverse directions. The top and bottom walls of the channel are assumed to be smooth; and depending on the configuration simulated, a no-slip or slip boundary condition is imposed on the fluid phase at the top wall. At the bottom wall a no-slip condition is employed for all simulations. Sediment particles are assumed to be fine enough to have zero net-deposition; thus a boundary condition was imposed which instantly re-entrains all settled sediment particles. For the channel flow configuration, the imposed boundary conditions are mathematically represented as

$$\tilde{u}_i = 0 \quad \text{at} \quad \tilde{z} = -1 \quad \text{and} \quad \tilde{z} = 1 \tag{8a}$$

$$\tilde{c}\tilde{V} + \frac{1}{Re_\tau Sc}\frac{\partial \tilde{c}}{\partial \tilde{z}} = 0 \quad \text{at} \quad \tilde{z} = -1 \quad \text{and} \quad \tilde{z} = 1 \tag{8b}$$

And for the open-channel like configuration, the imposed boundary conditions are

$$\tilde{u}_i = 0 \quad \text{at} \quad \tilde{z} = -1 \quad \text{and} \quad \frac{\partial \tilde{u}}{\partial \tilde{z}} = \frac{\partial \tilde{v}}{\partial \tilde{z}} = \tilde{w} = 0 \quad \text{at} \quad \tilde{z} = 1 \tag{9a}$$

$$\tilde{c}\tilde{V} + \frac{1}{Re_\tau Sc}\frac{\partial \tilde{c}}{\partial \tilde{z}} = 0 \quad \text{at} \quad \tilde{z} = -1 \quad \text{and} \quad \tilde{z} = 1 \tag{9b}$$

The boundary condition imposed for suspended sediment allows the net amount of sediment in suspension to remain constant through out the simulation. When integrated over time, the aforementioned condition allows the flow to reach a statistically steady state (Cantero et al., 2009).

ESURFD
1, 923–950, 2013

3 Results

Sixteen DNS simulations were run for the present study. They were all run for the same shear Reynolds number of 180, but different particle fall velocities ($\tilde{V}$) and shear Richardson number (Ri_τ). All the simulated cases have been listed in Table 1. The simulations can be broadly divided into two parts, twelve that were done with the channel flow configurations and four done with the boundary layer configuration.

3.1 Channel flow configuration

Among the twelve simulations done for the channel flow configuration, the first one was done without any suspended sediment. A set (*set1*) of simulations were done for constant shear Richardson number but increasing $\tilde{V}$. This set is equivalent to the situation where, the initial volume-averaged suspended sediment concentration is constant but the sediment particle size increases. The other set (*set2*) of simulations done for the same configuration is with a constant $\tilde{V}$ equal to 0.025 but increasing shear Richardson number. This set is equivalent to the situation where, the particle size of sediment is constant but the initial volume-averaged suspended sediment concentration increases. For both *set1* and *set2,* increase in $\tilde{V}$ or Ri_τ while keeping the other parameter constant results in an increase in the degree of stratification. Dutta (2012) showed that increase in either $\tilde{V}$ or Ri_τ increases the degree of self-stratification caused by suspended sediment and the extent to which a flow will stratify depends on the parameter $\tilde{V}Ri_\tau$. Cantero et al. (2012) made similar observations for turbidity currents.

In Figs. 2 and 3, we have plotted the mean streamwise velocity, steady state sediment concentration profile and normalized wall-normal turbulence intensity for *set1* and *set2*. For both the sets, increase in degree of self-stratification leads to increase in bulk streamwise velocity of the flow. The flow also becomes asymmetric, with the velocity maximum getting skewed towards the channel bottom. Even though the bulk streamwise velocity increases, turbulence intensity (W_{rms}) in the channel decreases, especially near the channel bottom. Flow in channel for different levels of self-stratification

ESURFD
1, 923–950, 2013

can be clearly divided into two regimes, first (for $\tilde{V}Ri_\tau \leq 0.36$) in which the turbulence near the bottom of the channel is damped but the flow in general is still turbulent. Second (for $\tilde{V}Ri_\tau \geq 0.45$) in which turbulence near the bottom of the channel is almost completely supressed, but turbulence intensity in the upper half of the channel is slightly more than the case with no suspended sediment. The steady state sediment concentration profiles in Figs. 2 and 3 are used with Eq. (5) to calculate vertical sediment diffusivity profiles (Fig. 4) for all the cases in *set1* and *set2*. Sediment diffusivity profiles are found to reflect the trends seen in the turbulence intensity profiles in Figs. 2 and 3. This result is along the expected lines, if we return to the exact definition of vertical sediment diffusivity, it is nothing but a surrogate used to model the vertical sediment flux due to turbulence ($\overline{w'c'}$). So wherever turbulence is damped, K_z/Hu_* decreases and wherever turbulence increases K_z/Hu_* also increases. Thus the mechanism through which self-stratification affects sediment diffusivity is equivalent to the mechanism through which it affects turbulence intensity.

3.2 Boundary layer configuration

Four numerical simulations were done for the boundary layer configuration. The boundary layer configuration is similar to the open-channel configuration but not exactly the same. Like the open-channel configuration, a slip boundary condition is imposed at the top wall for the fluid phase. In Fig. 5, bulk streamwise velocity, steady-state sediment concentration profile and normalized turbulence intensity have been plotted. The four simulations for the open-channel like configuration have the same particle fall velocity ($\tilde{V}$) but increasing shear Richardson number. Similar to the channel flow configuration, bulk streamwise velocity was found to increase with increase in shear Richardson number. Turbulence intensity was found to decrease with increase in shear Richardson number. And unlike the channel flow configuration where turbulence intensity decrease in the lower half of the channel and increase in the upper half; turbulence intensity was found to decrease throughout the channel. Though, the extent of damping in the upper half was found to be slightly more than the extent of damping in the lower half of the

ESURFD
1, 923–950, 2013

boundary layer. The steady state sediment concentration profiles in Fig. 5 were used to calculate vertical sediment diffusivity profiles (Fig. 6) for the four simulated cases. Reflecting the trend shown by turbulence intensity, vertical sediment diffusivity was found to decrease with increase in level of self-stratification. In the next section we discuss the larger implication of the observations made in the previous sections. We also address whether the observations made from the DNS results are reflected in experimental and field observations.

4 Discussion

In the preceding sections we saw how self-stratification due to suspended sediments can reduce sediment diffusivity in a flow. All the discussed results were on the basis of high-resolution numerical simulations, which were set up to exclusively capture the effect of self-stratification on sediment diffusivity. In order to vet our hypothesis against more realistic data, we compare our results to experimental observations of Ismail (1952) and Coleman (1986).

Ismail (1952) conducted a series of experiments in a closed rectangular channel. The aim of the experiments was to understand the transfer mechanism of turbulence and its interaction with suspended sediment. The rectangular closed channel setup is similar to our DNS simulations for the channel flow configuration. We have employed cases 74, 75, 76 and 78 from Ismail (1952). All the cases for which suspended sediment concentration profiles were available had dunes at the bottom of the channel, whereas for the numerical simulations we used smooth walls. This effect has been neglected for the purpose of qualitative comparison of the numerical results to experimental observations. Ismail (1952) also provides mean streamwise velocity profiles for few cases with and without sediment. We have reproduced cases 5 and 117 in this work. Figure 7a reflects the trend shown for streamwise velocity in the DNS results. Compared with the case without sediment, we clearly see in the case with sediment that streamwise velocity in the upper half of the channel increases whereas in the

ESURFD
1, 923–950, 2013

lower half decreases. Suspended sediment concentration profiles for cases 74–76 and 78 were used to calculate the sediment diffusivity profiles (Fig. 7b). All the cases used in the present study have been listed in Table 2; along with their corresponding shear Reynolds number, Ri_τ, $\tilde{V}$ and $\tilde{V}Ri_\tau$. The trend shown by sediment diffusivity calculated using data from Ismail's experiments is very similar to the one observed through the DNS results. Case 74 has the highest level of self-stratification ($\tilde{V}Ri_\tau$) and case 78 the lowest; and moving from case 78 to 74, vertical sediment diffusivity decreases in the lower half of the channel and increases in upper half of the channel. So, the results from the experiments concur with the trend we observed in the results from the DNS.

For comparing the boundary layer (open-channel like) case we use suspended sediment concentration profiles published by Coleman (1986). Coleman studied the effect of suspended sediment on the velocity-distribution of an open-channel flow. The effect of suspended sediment on the streamwise velocity is similar to the effect observed in our DNS results (Fig. 1 in Coleman, 1986). Coleman found that presence of suspended sediment slightly decreased the streamwise velocity near the bottom of the channel and slightly increased in the upper half of the channel. Increase in streamwise velocity in the upper portion of the boundary-layer is also consistent with observations by Barenblatt and Golitsyn (1974) for "mature dust storms". For the present study, we only used the suspended sediment concentration profiles for sediment of diameter (D) 0.210 mm. Coleman conducted his experiments for a particular sediment size and a constant hydraulic condition (constant slope and discharge), and he added sediment to the flow till the amount of sediment in the flow reached its maximum capacity. So, for a particular sediment size and flow condition, we have suspended sediment profiles for different net sediment concentration. The sediment concentration profiles were used to calculate vertical sediment diffusivity profiles (Fig. 8). The cases used for the present study have also been listed in Table 3, along with the corresponding $\tilde{V}$, Ri_τ and $\tilde{V}Ri_\tau$. As expected $\tilde{V}Ri_\tau$ increases from case 1 to case 10. In Fig. 8, we observe that in general vertical sediment diffusivity decreases with increase in $\tilde{V}Ri_\tau$, especially if you see the difference between case 1 and case 10. Although, the trend of decreasing sediment

ESURFD
1, 923–950, 2013

diffusivity with increase in $\tilde{V}Ri_\tau$ is not monotonic. We speculate that this is due to two competing effects trying to influence the sediment diffusivity in two opposite directions. It is known that sediment particles in suspension can increase turbulent kinetic energy (Niño and Garcia, 1998), which can then lead to higher sediment diffusivity; whereas increase in self-stratification tends to lower sediment diffusivity. Another factor that might be contributing to this slight inconsistency of the trend in the present case is irregularity of the $\tilde{V}$ values for different cases (refer to Table 3.). Even though theoretically all the cases should have the same $\tilde{V}$, the experimental observations actually have some inconsistencies (we have checked with a copy of the actual data set of N.L. Coleman). As change in $\tilde{V}$ has an influence on the mixing length of the fluid (Nielsen and Teakle, 2004), these small inconsistencies in $\tilde{V}$ might be obfuscating the expected trend of decrease of sediment diffusivity with an increase in $\tilde{V}Ri_\tau$. Even though sediment diffusivity in general decreases (see case 1 and case 10) with increase in self-stratification, the trend is not consistent. An important point to observe from the preceding discussions is that; along with the particle settling velocity ($\tilde{V}$), suspended sediment concentration (Ri_τ) is an important parameter that influences the degree of self-stratification in a sediment suspension. Amongst other mechanisms that increase sediment diffusivity with increase in $\tilde{V}$ (van Rijn, 1984; Nielsen and Teakle, 2004), increase in stratification due to suspended sediment decreases sediment diffusivity; and we think this can explain the aforementioned anomaly in the expected trend in Fig. 1.

5 Conclusions

In the present study we used sediment concentration profiles from Direct Numerical Simulations of sediment-laden flow through a channel, to calculate sediment diffusivity profiles for the channel flow and boundary-layer configuration. This allowed us for the first time to explicitly study the effect of sediment-induced stratification on sediment diffusivity. For the channel flow configuration, increase in stratification was found to decrease sediment diffusivity in the lower half of the channel and slightly increase sed-

ESURFD
1, 923–950, 2013

iment diffusivity in the upper half of the channel. For the boundary layer (open-channel like) configuration, throughout the channel sediment diffusivity was found to decrease with increase in stratification. Though, the extent of suppression of sediment diffusivity in the lower half of the boundary layer is appreciably lower than rest of the boundary layer. Along the expected lines, the sediment diffusivity profiles reflected the computed turbulence intensity profiles. Observations from the DNS results were vetted against experimental results of Ismail (1952) and Coleman (1986). Sediment diffusivity profiles calculated using concentration profiles from Ismail's closed channel experiments were found to be consistent with the DNS results. Sediment diffusivity profiles calculated using sediment concentration data from Coleman's (1986) experiments were more or less consistent with the DNS results, but the trend of decrease of sediment diffusivity with increase in stratification was erratic. For the present study we have only used one set of experiments of Coleman (1986); it would be interesting to repeat the calculations using data from rest of Coleman's (1986) experiments and other similar experiments. On the basis of our observations of the DNS and experimental results, we think a plausible explanation for the inconsistencies is sediment-induced stratification. A better understanding of sediment diffusivity and the various factors it depends on will eventually help us to ascertain suspended load in rivers/streams more accurately. At the end of the day, interaction between suspended sediment and the ambient fluid is highly nonlinear and will require further exploration to reveal more of its secrets.

Acknowledgements. We would like to thank Gary Parker, Carlos Pantano and Tzu-Hao Yeh for all the thought provoking and helpful discussions on the topic. This research was possible thanks to the Chester and Helen Siess Professorship in Civil Engineering at the University of Illinois. The support received by the junior author from a CSE Graduate Student Fellowship and the Ravindar K. and Kavita Kinra Fellowship in Civil and Environmental Engineering is gratefully acknowledged.

ESURFD
1, 923–950, 2013

References

Anderson, A. G.: Distribution of suspended sediment in a natural stream, EOS T. Am. Geophys. Un., 23, 678–683, 1942.

Barenblatt, G. I. and Golitsyn, G. S.: Local structure of mature dust storms, J. Atmos. Sci., 31, 1917–1933, 1974.

Bennett, S. J., Bridge, J. S., and Best, J. L.: The fluid and sediment dynamics of upper-stage plane beds, J. Geophys. Res.-Oceans, 103, 1239–1274, 1998.

Cantero, M. I., Balachandar, S., and Garcia, M. H.: An Eulerian-Eulerian model for gravity currents driven by intertial paritcles, Int. J. Multiphas. Flow, 34, 484–501, 2008.

Cantero, M. I., Balachandar, S., and Parker, G.: Direct Numerical Simulation of stratification effects in a sediment-laden turbulent channel flow, J. Turbul., 10, N27, doi:10.1080/14685240903159197, 2009.

Cantero, M. I., Shringarpure, M., and Balachandar, S.: Towards a universal criteria for turbulence suppression in dilute turbidity currents with non-cohesive sediments, Geophys. Res. Lett., 39, L14603, doi:10.1029/2012GL052514, 2012.

Coleman, N. L.: Flume studies of the sediment transfer coefficient, Water Resour. Res., 6, 801–809, 1970.

Coleman, N. L.: Effects of suspended sediment on the open-channel velocity distribution, Water Resour. Res., 22, 1377–1384, 1986.

Dutta, S.: Effect of self-stratification on channel flows and boundary layers: a study using direct numerical simulations, MS thesis, University of Illinois at Urbana-Champaign, USA, 2012.

Ferry, J. and Balachandar, S.: A fast Eulerian method for disperse two-phase flow, Int. J. Multiphas. Flow, 27, 1199–1226, 2001.

Garcia, M. H. (Ed.): Manual 110. Sedimentation Engineering: Processes, Measurements, Modelling and Practice, ASCE, 46, Reston VA, USA, 2008.

Ismail, H. M.: Turbulent transfer mechanisms and suspended sediment in closed channels, T. Am. Soc. Civ. Eng., 117, 409–434, 1952.

Nielsen, P.: Coastal Bottom Boundary Layer and Sediment Transport, World Scientific, River Edge NJ, USA, 1992.

Nielsen, P. and Teakle, I. A. L.: Turbulent diffusion of momentum and suspended particles: a finite-mixing-length theory, Phys. Fluids, 16, 2342–2348, 2004.

ESURFD
1, 923–950, 2013

Niño, Y. and Garcia, M. H.: On Engelund's analysis of turbulent energy and suspended load, J. Eng. Mech.-ASCE, 124, 480–483, 1998.
Segre, P. N., Liu, F., Umbanhowar, P., and Weltz, D. A.: An effective gravitational temperature for sedimentation, Nature, 409, 594–597, 2001.
Smith, J. D. and McLean, S. R.: Spatially averaged flow over a wavy surface, J. Geophys. Res., 82, 1735–1746, 1977.
Shringarpure, M., Cantero, M. I., and Balachandar, S.: Dynamics of complete turbulence suppression in turbidity currents driven by monodisperse suspensions of sediment, J. Fluid Mech., 712, 384–417, 2012.
Rouse, H.: Modern conceptions of the mechanics turbulence, T. Am. Soc. Civ. Eng., 102, 463–543, 1937.
Van Rijn, L. C.: Sediment transport, Part II: Suspended load transport, J. Hydraul. Eng.-ASCE, 110, 1613–1641, 1984.
Vanoni, V. A.: Transportation of sediment by water, EOS T. Am. Geophys. Un., 3, 67–133, 1946.
Wright, S. and Parker, G.: Density stratification effects in sand-bed river, J. Hydraul. Eng.-ASCE, 130, 783–795, 2004.

ESURFD
1, 923–950, 2013

Table 1. The table lists all the cases of Direct Numerical Simulations used in the current study. All the simulations have the same Re_τ. Cases 1 to 12 correspond to the simulations for channel configuration and 13 to 16 correspond to the simulations for open-channel like configuration. Case 1 corresponds to the case with no sediment in suspension, and was simulated to compare with the self-stratified cases.

Case	Re_τ	$\tilde{V} = V/u_*$	Ri_τ	Configuration
1	180	0	0	channel
2	180	0.005	18	channel
3	180	0.01	18	channel
4	180	0.015	18	channel
5	180	0.02	18	channel
6	180	0.025	18	channel
7	180	0.03	18	channel
8	180	0.025	1	channel
9	180	0.025	10	channel
10	180	0.025	15	channel
11	180	0.025	20	channel
12	180	0.025	22	channel
13	180	0.025	1	Blayer
14	180	0.025	10	Blayer
15	180	0.025	15	Blayer
16	180	0.025	18	Blayer

ESURFD
1, 923–950, 2013

Table 2. The table lists all the experiments of Ismail (1952) we have used in the present study.

Case	Re_τ	$\tilde{V} = V/u_*$	Ri_τ	$\tilde{V}Ri_\tau$
74	1409	0.25	3.629	0.90723
75	1546	0.197	4.426	0.87192
76	1978	0.176	3.192	0.56179
78	2698	0.133	1.729	0.22996
5	1768	0	0	0
117	2188	0.359	2.926	1.05043

ESURFD
1, 923–950, 2013

Table 3. The table lists all the experiments of Coleman (1986) we have used in our study.

$Re_\tau = 3700$		$D = 0.210\,\text{mm}$	
	Ri_τ	$\tilde{V} = V/u_*$	$\tilde{V}Ri_\tau$
1	0.2005	0.606	0.1215
2	0.4583	0.606	0.2778
3	0.6631	0.606	0.4018
4	1.0221	0.622	0.6358
5	1.1773	0.569	0.6699
6	1.5287	0.599	0.9157
7	1.6615	0.598	0.9936
9	2.0140	0.605	1.2185
10	2.2193	0.607	1.3471

ESURFD
1, 923–950, 2013

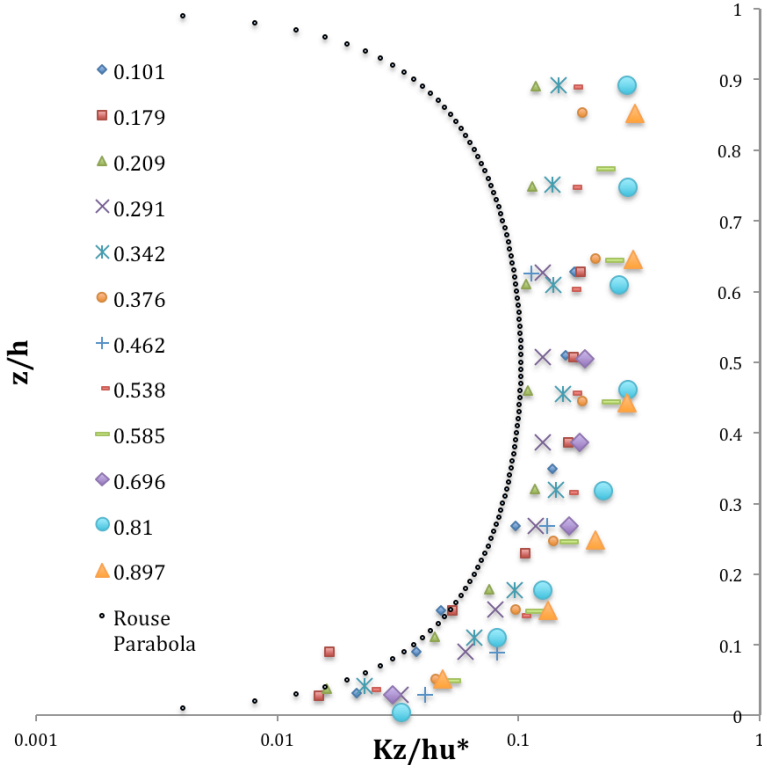

Fig. 1. Vertical sediment diffusivity K_z/Hu_* profiles for sediments with different $\tilde{V} = V/u_*$. The data has been reproduced from calculations done by Coleman (1970) on field data of Anderson (1942). The generic Rousian profile of kinematic eddy viscosity has also been plotted. For most cases the Rousian profile underestimates sediment diffusivity. There is a trend that vertical sediment diffusivity increases with increase in $\tilde{V}$; but the trend is not very obvious for some of the cases plotted above (e.g. between 0.585 and 0.696).

ESURFD
1, 923–950, 2013

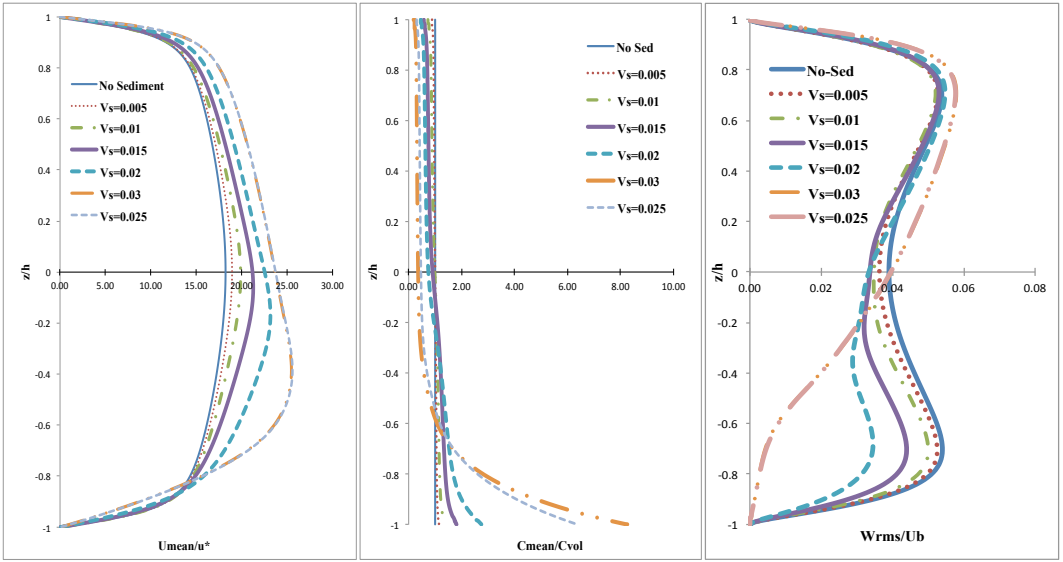

Fig. 2. Results from the DNSs in a channel flow setting, for increasing $\tilde{V}$ and $Ri_\tau = 18$. Mean streamwise velocity and asymmetry of the flow increases with increase in $\tilde{V}$. Increase in $\tilde{V}$ increases the degree of self-stratification of the flow; this leads to increase in sediment concentration gradient and higher amount of turbulence damping near the channel bottom. In the channel normalized turbulence intensity (W_{rms}/U_b) is modulated, with decrease in lower half of the channel and slight increase in the upper half of the channel.

ESURFD
1, 923–950, 2013

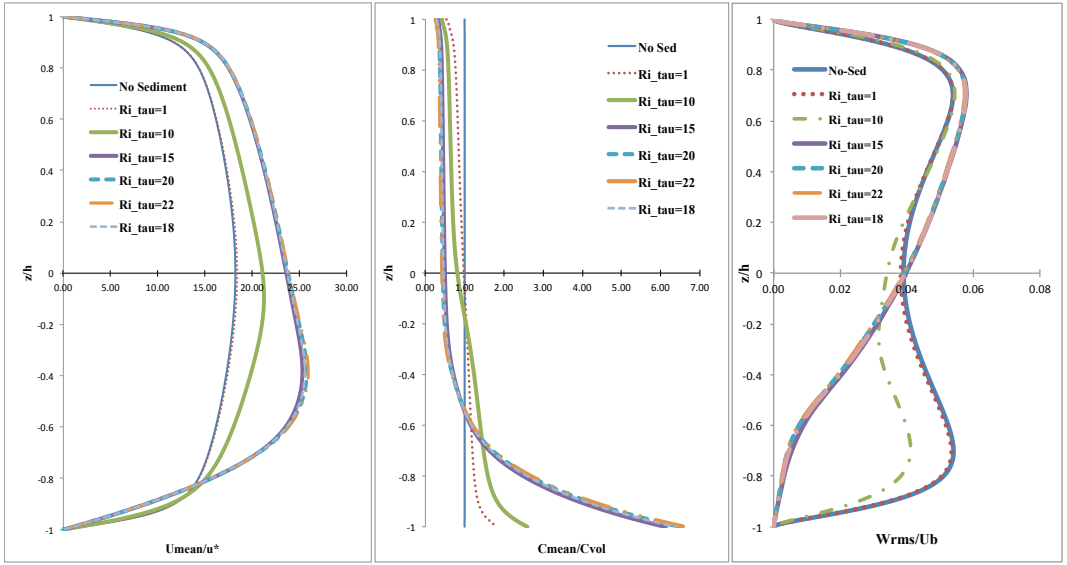

Fig. 3. Results from the DNSs in a channel flow setting, for increasing Ri_τ and $\tilde{V} = 0.025$. Mean streamwise velocity and asymmetry of the flow increases with increase in Ri_τ. Increase in Ri_τ increases the degree of self-stratification of the flow; this leads to increase in sediment concentration gradient and higher amount of turbulence damping near the channel bottom. In the channel normalized turbulence intensity (W_{rms}/U_b) is modulated, with decrease in lower half of the channel and slight increase in the upper half of the channel.

ESURFD
1, 923–950, 2013

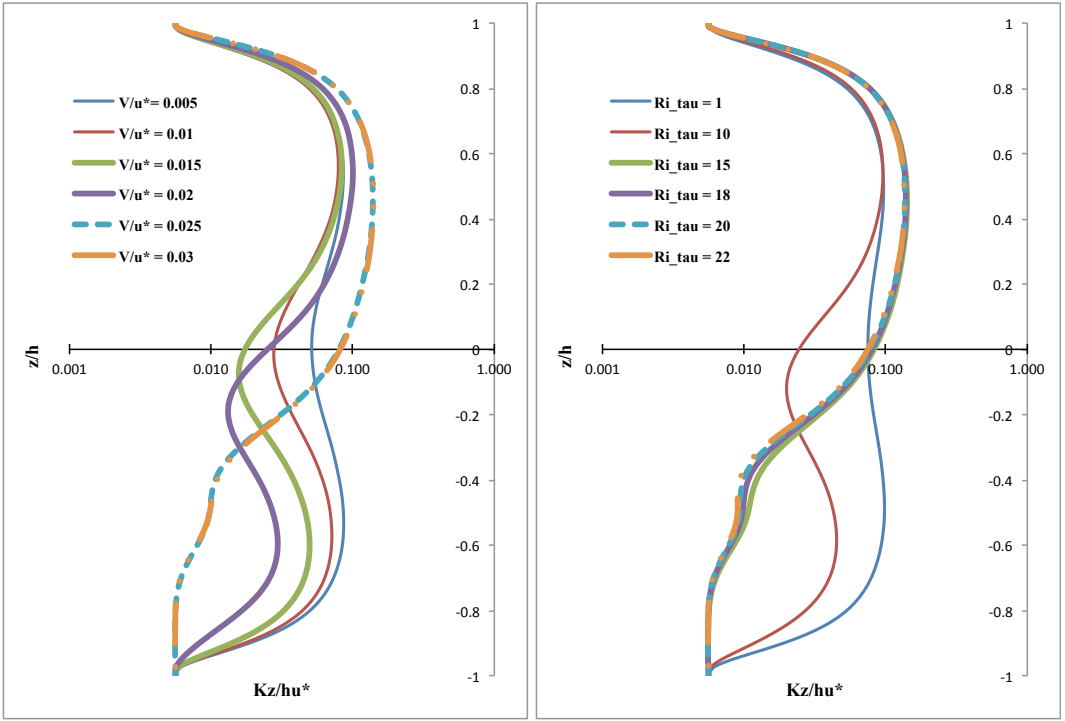

Fig. 4. The trend for vertical sediment diffusivity mirrors the trend found for turbulence intensity. Increase in degree of self-stratification is found to decrease sediment diffusivity in the lower half of the channel and increase sediment diffusivity in the upper half of the channel. This is not completely unexpected because mixing of suspended sediment is primarily dependent on turbulence in the flow.

ESURFD
1, 923–950, 2013

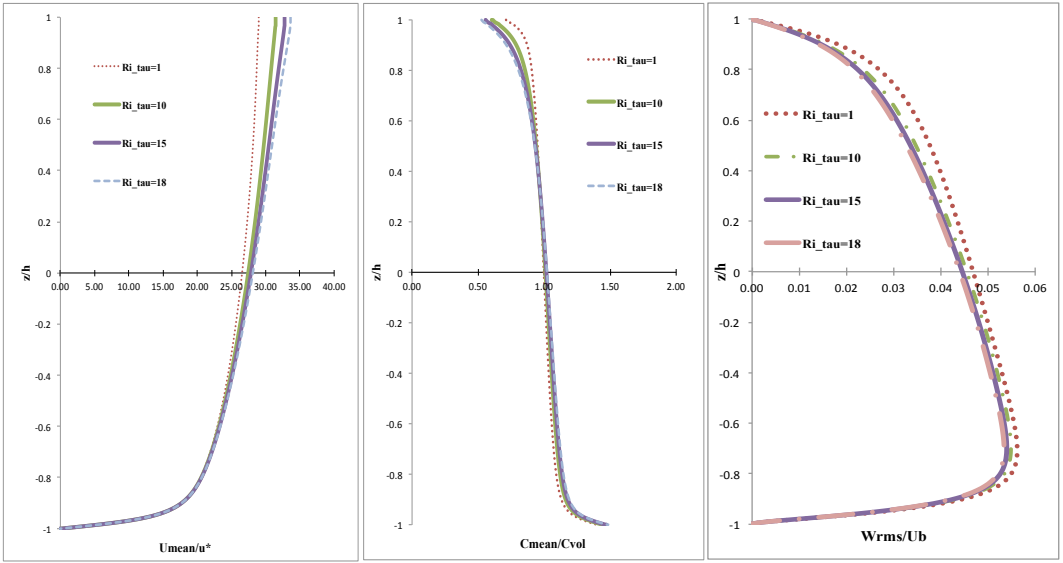

Fig. 5. Results from the DNSs in a boundary layer (open-channel like) setting, for increasing Ri_τ and $\tilde{V} = 0.025$. Mean streamwise velocity of the flow increases with increase in Ri_τ. Increase in Ri_τ increases the degree of self-stratification of the flow; this leads to increase in sediment concentration gradient and higher amount of turbulence damping through out the domain. Normalized turbulence intensity (W_{rms}/U_b) is damped throughout the boundary layer but the level of suppression is slightly higher in the upper half.

ESURFD
1, 923–950, 2013

Effect of self-stratification on sediment diffusivity

S. Dutta et al.

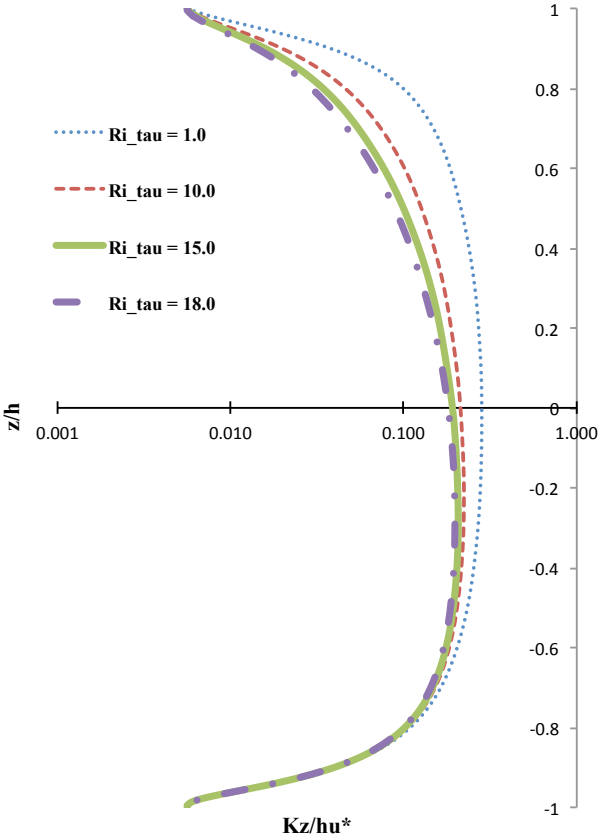

Fig. 6. The trend for vertical sediment diffusivity mirrors the trend found for turbulence intensity. Increase in degree of self-stratification is found to decrease sediment diffusivity in the boundary layer. The extent to which sediment diffusivity decreases in the upper half of the boundary layer is slightly higher than the lower half of the boundary layer. This is not completely unexpected because mixing of suspended sediment is primarily dependent on turbulence in the flow.

ESURFD
1, 923–950, 2013

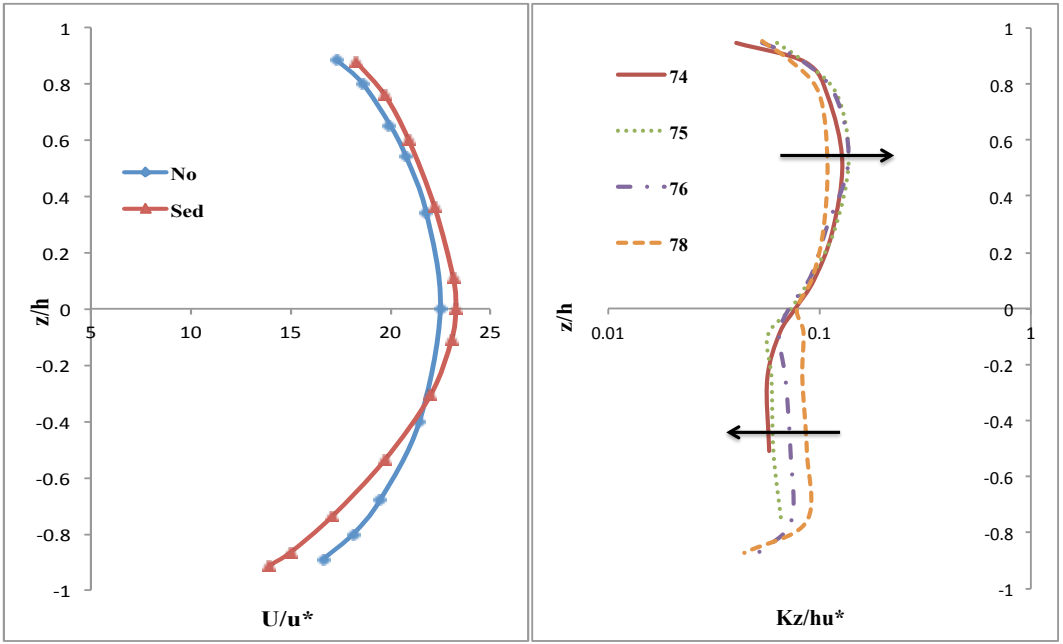

Fig. 7. Streamwise velocity for cases 5 and 117 has been reproduced from Ismail (1952). Case 5 has no sediment in suspension and case 117 has suspended sediment. Vertical sediment diffusivity for cases 74–76, 78 was calculated from sediment concentration profiles from experiments performed by Ismail (1952). With increase in $\tilde{V}Ri_{\tau}$, vertical sediment diffusivity in the channel slightly increases in top half of the channel and decreases in the lower half of the channel; and this completely agrees with the DNS results.

ESURFD
1, 923–950, 2013

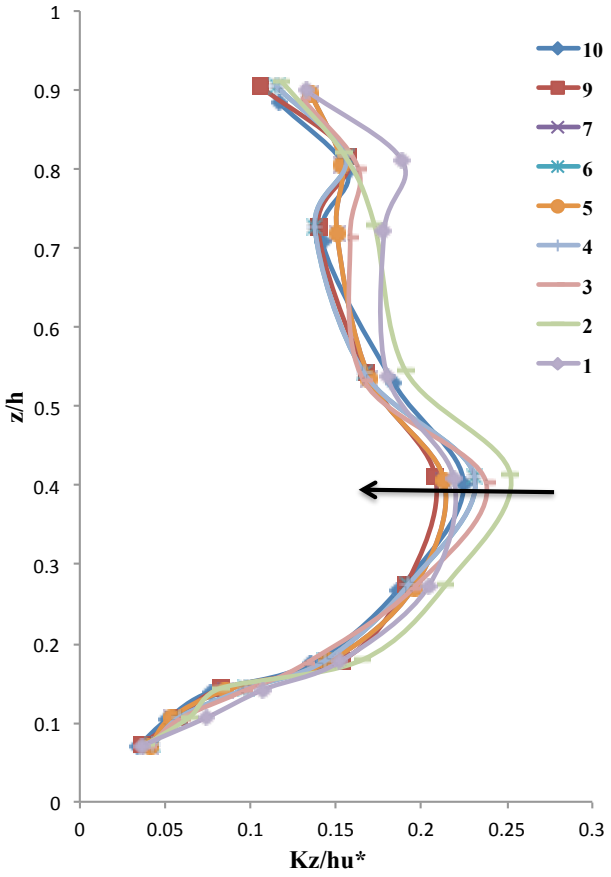

Fig. 8. Vertical sediment diffusivity was calculated using sediment concentration profiles from experiments performed by Coleman (1986). With increase in $\tilde{V}Ri_\tau$ (case 1 to 10), vertical sediment diffusivity in the open-channel flow decreases.

ESURFD
1, 923–950, 2013

Effect of self-stratification on sediment diffusivity

S. Dutta et al.